Application of Active Disturbance Rejection Control (ADRC) in the Radial Position Control of a Bearingless Induction Machine With Split Winding

Werbet L. A. Silva[1]*, Elmer R. L. Villarreal[2]†, Jossana M. S. Ferreira[1]‡, José A. Paiva[3]§, Andrés O. Salazar[1]¶ and Andre L. Maitelli[1]‖

[1] Universidade Federal do Rio Grande do Norte, Natal-RN, Brazil
werbethluizz@hotmail.com
jossana@ect.ufrn.br
maitelli@dca.ufrn.br
andres@dca.ufrn.br
[2] Universidade Federal Rural do Semi-Árido, Mossoró-RN, Brazil.
elmerllanos@ufersa.edu.br
[3] Instituto Federal de Educação, Ciência e Tecnologia do Rio Grande do Norte, Natal-RN, Brazil.
jalvaro.paiva@gmail.com

Abstract

In this work, the Active Disturbance Rejection Control (ADRC) technique was applied to control a simulated plant that represents the radial displacement of a bearingless induction machine with split winding. Active Disturbance Rejection Controllers have a robust operation when applied to systems with uncertainties, nonlinearities, and in the presence of disturbances. The work employed the linear and nonlinear versions of the ADRC to control the radial displacement. The simulations were performed in the Scilab software. The system response under parameter variation and external load are presented to compare the performance and implementation of both techniques.

1 Introduction

The emergence of electrical machines with magnetic suspension of the rotor meets industry demand for motors that could generate less noise, reach higher speeds and avoid process contamination. In the past two decades, magnetic bearing technology has received significant attention due to its potential application to high-speed and harsh environments applications, where maintenance routines are more complicated. In this way, different machine types have been tested under the magnetic suspension scheme, and new structures appeared to overcome the natural problems of this technology.

Electrical machines that combine motor functions for torque generation and magnetic bearings in the same system, known as bearingless machines, are considered the greatest advance in this area of knowledge [10][13]. The bearingless technology has been applied in different electrical machine types; the induction motor, e.g., is often chosen due to its robustness, simplicity, and low cost [17][1][20]. [12] proposed a bearingless induction motor in which the group of

*Designed and implemented the control system
†Run simulations and tests and studied the model
‡Did numerous tests and provided a lot of suggestions
§Did the literature review and o wrote the main sections
¶Literature, text review and orientation
‖Literature, text review and orientation

coils that generate rotational torque also generates radial forces. This structure, known as split winding, aims to simplify the operation and improve the internal use of space of the motor. The same approach was used by [2] to propose the use of split windings in a traditional three-phase induction motor, obtaining a system capable of generating greater radial forces.

Since the magnetic shaft suspension is a naturally unstable system, the bearingless machine strongly depends on well-designed control routines. These systems are multivariable, non-linear, and coupled [20]. So linear position controllers, as the Proportional-Integral-Derivative (PID) [11], may not achieve a response fast and stable enough for proper shaft suspension. The use of microprocessors and power electronics devices enabled the application of advanced control theories, such as predictive control, sliding mode control, neural network control, Fuzzy control, and others [19]. In recent years, the Active Disturbance Rejection Control (ADRC) "is emerging as a promising alternative in many tough control scenarios, due to its structure simplicity and capability in dealing with the model uncertainties, nonlinearity and external disturbances within a unified framework" [16].

The ADRC has been widely studied in virtue of its anti-disturbance ability and its independence of a precise system model [6]. Its main idea is to group all the uncertainties of the plant – such as non-modeled dynamics, external disturbances, and variations in parameters – as an additional state variable to be estimated in real-time through the input and output variables. Thus, the additional state can be estimated and compensated in the control loop. This task is achieved thanks to the core element of the ADRC: the Extended State Observer (ESO). Employing the ESO, the output and its derivatives, as well as the lumped disturbance, the desired control performance can be achieved by a simple linear state feedback control algorithm with online disturbance rejection [18]. This works aims to apply the ADRC technique to control the rotor radial position of a four-pole bearingless induction machine with split winding.

The original concept of the ADRC controller proposed a completely non-linear structure. Despite being very efficient for non-linear systems, this structure is relatively complicated to be tuned because it has a large number of parameters. Gao's work sought to obtain a linear model of the ADRC controller that would maintain the good performance of the original controller.

This work is the first stage of a project that aims to apply the ADRC controller in the radial position control of an induction bearingless machine with split coil. Initially, we simulated the application of a linear and a non-linear ADRC structure to control a radial position system in order to understand the implementation, evaluate advantages and disadvantages, and assess the performance of the closed-loop control system. These results are the grounding foundation for the following stages of the project.

The results of these experiments are described in this text, which is organized as follows: in addition to this introductory section, section 2 provides a brief presentation of the radial displacement model used; section 3 describes the linear and non-linear structures of ADRC; section 4 shows the results of the simulations; finally, the conclusion section shows the most important points that were evaluated from this work.

2 Bearingless machine with split winding

2.1 Operation principle

In the stator of a three-phase bearing motor, there are three groups of windings divided to generate radial force and torque. The coils are split in the stator as shown in Figure 1. Considering a four-pole three-phase motor, Figure 2 can be used to explain the principle of generating radial magnetic forces in the rotor.

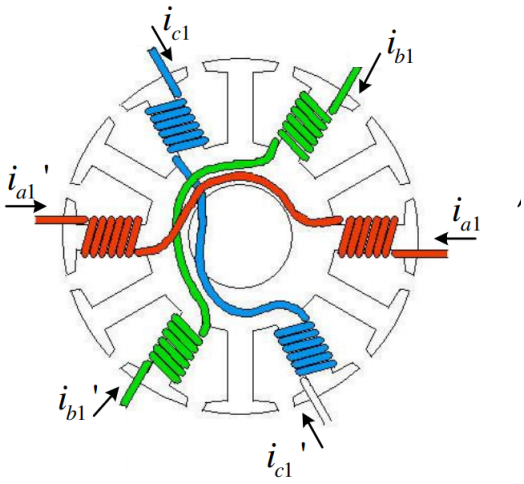

Figure 1: Winding's distribution.

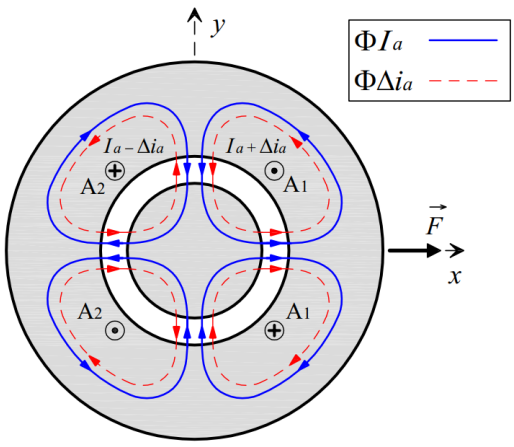

Figure 2: Radial forces generation.

Phase A is divided into two groups of coils: A1 and A2. When the same current (I_a) flows through coils A1 and A2, a magnetic flux is created, as represented in Figure 2 by solid blue lines. When the current increases by Δi_a in coil A1 and simultaneously decreases by Δi_a in coil A2, the flux density increases on one side of the rotor while it decreases on the opposite direction with the same magnitude. The unbalance in the original flux generated by Δi_a generates radial force in the positive direction of the axis X. Likewise, it occurs in the opposite direction when the additional current is added to coil A2 and subtracted from coil A1.

Extending this mode of operation to the three phases and decomposing the coordinate system of the position of the coils as shown in Figure 1 in the coordinate system xy, it is possible to control the radial position in the entire bounded plane for xy.

2.2 Radial displacement model

This prototype works vertically and is supported on the lower end of the shaft by a pivoted bearing that prevents radial and axial movements, but allows angular movements. This type of system has two degrees of freedom for position control and the rotor displacement occurs in the directions of x and y axes.

From the application of the second motion law to Figure 3, [15] developed a linear dynamical representation for the rotor radial displacement system:

$$\ddot{y} = 8374y + 3680000u + w \tag{1}$$

where y is the radial position, u is the input current signal that can vary from $-1A$ to $1A$ and w is an output disturbance. In the form of a transfer function that relates the control signal $U(s)$ to the output position $Y(s)$ of the rotor, the dynamics of the x-axis is equal to the y-axis and both are described by:

$$G(s) = \frac{3.68 \times 10^6}{(s + 91.51)(s - 91.51)} \tag{2}$$

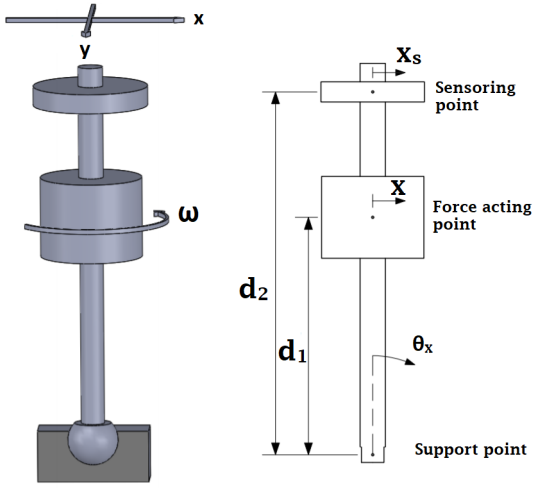

Figure 3: Rotor free body diagram.

Equation (2) shows that the radial position model has an unstable pole, thus a controller is fundamental to the system operation.

3 Active Disturbance Rejection Controller

The first version of the ADRC was presented in Chinese by its creator, Jingqing Han, in the work entitled "Auto disturbances rejection controller and its applications" in 1998 [7]. To promote advances in the theory and practice of control engineering, Jingqing Han researched the characteristics of nonlinear elements into closed-loop control problems and proved the efficiency of the controllers designed from them. According to [9], when compared to linear functions, nonlinear ones are potentially more effective in tolerating uncertainties and disturbances as well in improving systems dynamics.

In a more recent publication, Han described the ADRC as a digital closed-loop control technique, rooted in computer simulations, which inherits from the proportional-integral-derivative (PID) controller its characteristic of greatest success: a control law mainly based on error, and not just on the plant model; in addition, it uses state observers, a technique from the theory of modern controllers; and also makes use of nonlinear control tools for the realization of its structure [5].

Aiming to simplify the ADRC controller, [4] used only linear gains to propose a kind of linear ADRC that uses concepts of controller scaling and parameterization to make the controller parameters functions of the closed-loop bandwidth of the system. The version is called Linear ADRC (LADRC) and brought a new perspective to the industrial application of the technique once it maintained the controller abilities in rejecting disturbances and simplified the tuning process.

Both versions of ADRC (NADRC and LADRC) have exactly the same operation idea: using two control loops to emulate a simplified system, similar to a system composed only by cascaded integrators, in which the dynamic behavior can be controlled by a simple control law (feedback loop). To reach this task, an extended state observer estimates any unknown information (dynamics, disturbances, nonlinearities, parameter variations, time-delays, etc) by

the input-output data of the controlled system and removes this information in the control loop (feedforward loop). This structure makes the ADRC independent of the plant model, where the same structure can handle a large variety of dynamic systems. Furthermore, a Reference Generator can be used to provide a smooth version of the reference and its derivatives. This structure is shown in Figure 4.

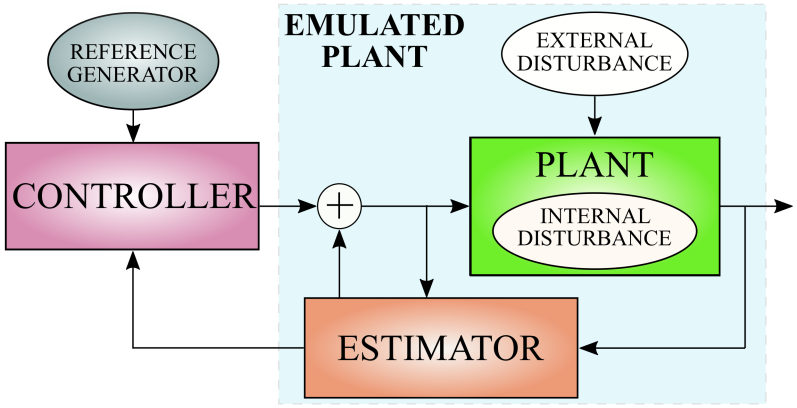

Figure 4: ADRC general idea.

The relative order of the plant is the only information necessary to build a controller based on ADRC. This information is needed because all the blocks described in Figure 4 are designed according to a specific dynamical order behavior. The following sections describe the design of the NADRC and the LADRC to a second-order system, once this is the relative order of our plant.

3.1 ADRC Structure

The mathematical description of the ADRC is based on [4]. A generic second-order system, to be controlled with ADRC, is represented by the following differential equation:

$$\ddot{y} = -a\dot{y} - by + w + bu \tag{3}$$

y is the output; u is the input; w represents an external disturbance; a and b are system parameters.

To apply the ADRC technique, there must be some information about the b parameter. Assuming an approximate value given by $b \approx b_0$, equation 3 can be rewritten as follows:

$$\ddot{y} = -a\dot{y} - by + w + (b - b_0)u + b_0u = f + b_0u \tag{4}$$

The term f in the above equation is denoted by generalized disturbance and is equal to $f = -a\dot{y} - by + w + (b - b_0)u$. The term $b - b_0$ represents the difference between the actual value of b and the approximation b_0, which must be specified to implement the algorithm. In state space form, assuming that $x_1 = y$ and $x_2 = \dot{x}_1$ the system given by 4 can be represented by:

$$\begin{cases} \dot{x}_1 = x_2 \\ \dot{x}_2 = b_0u + f \\ y = x_1 \end{cases} \tag{5}$$

Assuming that f can be estimated, the ADRC technique cancels its effect on the system output by applying the following relationship to the control loop:

$$u = \frac{u_0 - f(t)}{b_0} \tag{6}$$

Hence the total (emulated) dynamics of the system 5 becomes:

$$\begin{cases} \dot{x}_1 = x_2 \\ \dot{x}_2 = u_0 \\ y = x_1 \end{cases} \tag{7}$$

This is a simple double integrator system, whose control has been widely performed in the literature.

The concepts described above indicate that an estimation method that provides an accurate approximation of the value of f is fundamental for an adequate application of the ADRC technique. Furthermore, the control block must be able to meet performance expectations dynamic. The following sections describe two possible frameworks for fully implementing an ADRC-based controller.

3.2 NADRC Structure

The nonlinear structure of an ADRC controller is usually composed by three blocks: a Tracking Differentiator (TD), an Extended State Observer (ESO), and the nonlinear controller (Figure 5).

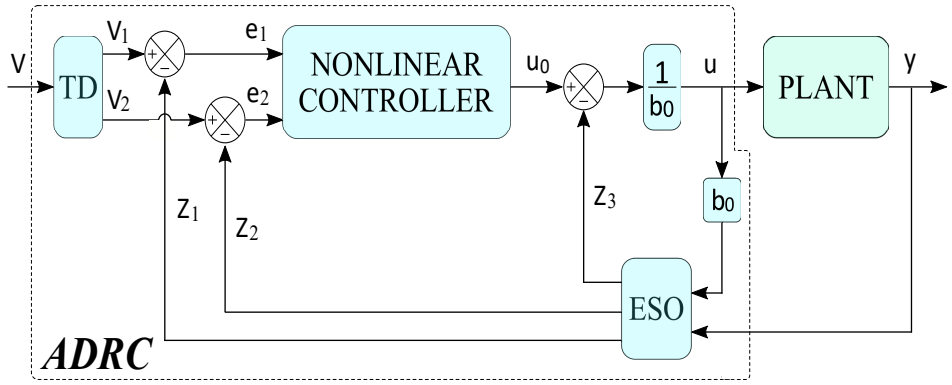

Figure 5: ADRC control loop structure.

3.2.1 Tracking Differentiator

The TD can be seen as a reference generator. It provides smooth versions of the reference signals that usually are put on the system input as a step function. Furthermore, it provides derivatives of the input without the noisy amplification of the traditional derivatives operations. For a second-order system given by:

$$\begin{cases} \dot{v}_1 = v_2 \\ \dot{v}_2 = u \end{cases} \tag{8}$$

an optimal solution is given by:

$$u = -rsign(v_1 - v + \frac{v_2|v_2|}{2r}) \tag{9}$$

This solution is named optimal because it can make the output of 8 reach the desired input fast and with low overshoot. The system can be rewritten as:

$$\begin{cases} \dot{v}_1 = v_2 \\ \dot{v}_2 = -rsign(v_1 - v(t) + \frac{v_2|v_2|}{2r}) \end{cases} \tag{10}$$

thus, $v_1(t)$ follows the input signal $v(t)$ with a speed adjusted by r. The variable $v_2 = \dot{v}_1$ is an approximation of the derivative of $v(t)$. The *sign* is given by:

$$sgn(e) = \begin{cases} 1, & e \geq 0 \\ -1, & e < 0 \end{cases} \tag{11}$$

3.2.2 Nonlinear Extended State Observer

The ESO is the most important block of the ADRC. In its structure the generalized disturbance f is considered as an additional state of the system 5:

$$\begin{cases} \dot{x}_1 = x_2 \\ \dot{x}_2 = x_3 + b_0 u \\ \dot{x}_3 = h \\ y = x_1 \end{cases} \tag{12}$$

where $x_3 = f$ is the augmented state and $h = \hat{f}$, its derivative. h is seen as an unknown disturbance. The above system can be rewritten by:

$$\begin{aligned} \dot{x} &= Ax + Bu + Eh \\ y &= Cz \end{aligned} \tag{13}$$

where:

$$\mathrm{A} = \begin{bmatrix} 0 & 1 & 0 \\ 0 & 0 & 1 \\ 0 & 0 & 0 \end{bmatrix}, \mathrm{B} = \begin{bmatrix} 0 \\ b_0 \\ 0 \end{bmatrix}, \mathrm{C} = \begin{bmatrix} 1 & 0 & 0 \end{bmatrix}, \mathrm{E} = \begin{bmatrix} 0 \\ 0 \\ 1 \end{bmatrix}$$

From the augmented system 12, it is possible to construct an observer to estimate numerical values to z_1, z_2 e z_3, which are the estimated values of the states x_1, x_2 e x_3. The work [3] proposed a nonlinear structure in which the ESO is such as:

$$\begin{aligned} \dot{z}_1 &= z_2 - \beta_1 fal(e, \alpha_1, d_1), \\ \dot{z}_2 &= z_3 - \beta_2 fal(e, \alpha_2, d_2) + b_0 u \\ \dot{z}_3 &= -\beta_3 fal(e, \alpha_3, d_3), \end{aligned} \tag{14}$$

where β_1, β_2 and β_3 are the observer gains of the nonlinear fal functions, whose definition is given by:

$$fal(e, \alpha, d) = \begin{cases} |e|^{\alpha} sgn(e), & |e| > d \\ \frac{e}{d^{1-\alpha}}, & |e| \leq d \end{cases} \tag{15}$$

the value of e is the error between the system output and its estimate $(\hat{y} - y)$ and α and d are tuning parameters.

3.2.3 Nonlinear Control Law

Among the control law alternatives proposed by [5], we can highlight the following:

$$u_0 = -K_P fal(e_1, \alpha_4, d_4) - K_D fal(\dot{e}_1 \alpha_5, d_5) \tag{16}$$

where e_1 is the error signal from the difference between the reference and the system output; K_P and K_D are gains; α_4, α_5, d_4, and d_5 are tuning parameters.

3.3 LADRC

Since there is no linear implementation of the Tracking Differentiator on the LADRC version proposed by [4], only the linear ESO and control law of the LADRC are described below.

3.3.1 LESO

The linear ESO proposed by [4] is built by removing the nonlinear terms of 14, such as:

$$\begin{cases} \dot{z}_1 = z_2 - \beta_1 e \\ \dot{z}_2 = z_3 - \beta_2 e + b_0 u \\ \dot{z}_3 = -\beta_3 e \end{cases} \tag{17}$$

where $e = (z_1 - y)$. This is equivalent to a tradicional Luenberger observer and can be rewritten as:

$$\begin{aligned} \dot{z} &= Az + Bu - L(\hat{y} - y) \\ \hat{y} &= Cz \end{aligned} \tag{18}$$

where the vector L if composed by the observer gains:

$$\mathrm{L} = \begin{bmatrix} \beta_1 & \beta_2 & \beta_3 \end{bmatrix}^T$$

These gains can be found by any method of pole allocation. In order to simplify the determination of the gains of the vector L, the tuning method proposed by [4] allocates all the poles in $-\omega_0$. ω_0 is assumed as the bandwidth of the observer. Solving $|s\mathbf{I} - (\mathbf{A} - \mathbf{LC})| = (s + \omega_0)^3$ gives:

$$\mathrm{L} = \begin{bmatrix} 3\omega_0 & 3\omega_0^2 & \omega_0^3 \end{bmatrix}^T$$

This procedure offers a systematic way to obtain the tuning parameters of the LESO. The ESO has advantages over nonlinear ESO considering the control complexities [8].

3.3.2 Linear Control Law

The state feedback method can be applied to control the emulated system of the LADRC. Considering the feedback law $u = -Kx$ gives:

$$u_0 = -K_1(r - z_1) - K_2(r - z_2) \tag{19}$$

K_1 and K_2 are the controller gains. The closed loop poles can be found by the allocation of all poles in $-\omega_c$. Solving $|s\mathbf{I} - (\mathbf{A} - \mathbf{BK})| = (s + \omega_c)^2$ and putting the gains grouped in a vector K:

$$\mathrm{K} = \begin{bmatrix} \omega_c^2 & 2\omega_c \end{bmatrix}$$

As for the ESO, the control law of the LADRC has a systematic way to tune the controller parameters.

4 Results

We simulated the control of the plant given by (2) using LADRC and NADRC to compare the performance of both techniques. For the results described in this section, the following considerations must be made:

- Since the dynamic response for the x and the y axis are equal, the results for only one axis are shown;
- The control goal is to maintain the radial position of the machine's rotor in $(x = 0, y = 0)$ position, so the reference signal v is kept in 0 and the Tracking Differentiator is not needed. Therefore the control loop implemented is showed on the Figure 6.

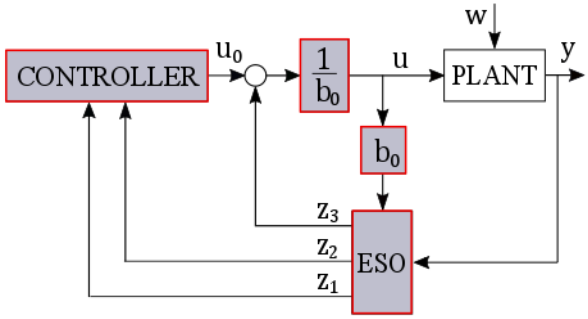

Figure 6: Control loop.

- The nonlinear ADRC was implemented using the equations (14) and the control law is given by (16);
- The linear ADRC was implemented using the equations (17) and the control law is given by (19);
- The controllers tuning was carried out by trial and error;
- The initial conditions are $x_1(0) = 1$ and $x_2(0) = 0$. This situation indicates that the machine rotor was stopped in an unwanted position before the controller starts acting;
- Two step-shaped disturbances were added at the output of the system at the instants $t = 0.1$ and $t = 0.3$ seconds. In a practical situation, disturbances of this type are caused by loads added to the axis of the machine in operation.
- Parameters variations in practice usually come from the natural heat by Joule effect of the circuits and power supplies. This condition is simulated in this work changing the plant dynamic according to:

$$\ddot{y} = (8374 + 8374 * 10 * t)y + 3680000u + w \tag{20}$$

Tables 1 and 2 show the controllers parameters used in the simulations for the LADRC and NADRC. The gains of the nonlinear ADRC blocks used the same of the LADRC.

Parameter	Value
step-size	0.0001 s
$x_1(0)$	1
$x_2(0)$	0
ω_c	147
ω_0	$5 * \omega_c$
b_0	2000000

Table 1: LADRC parameters.

Parameter	Value
step-size	0.0001 s
$x_1(0)$	1
$x_2(0)$	0
K_p	ω_c^2
Kd	$2\omega_c$
β_1	$3\omega_0$
β_2	$3\omega_0^2$
β_3	ω_0^3
b_0	2000000
$fal - ESO$	$d = 0,5;\ \alpha = 0,5$
$fal - Controller$	$d = 2;\ \alpha = 2$

Table 2: NADRC parameters.

Figure 7 shows the plant output for the two versions of the ADRC controller and the detailed views of relevant regions of the dynamical response.

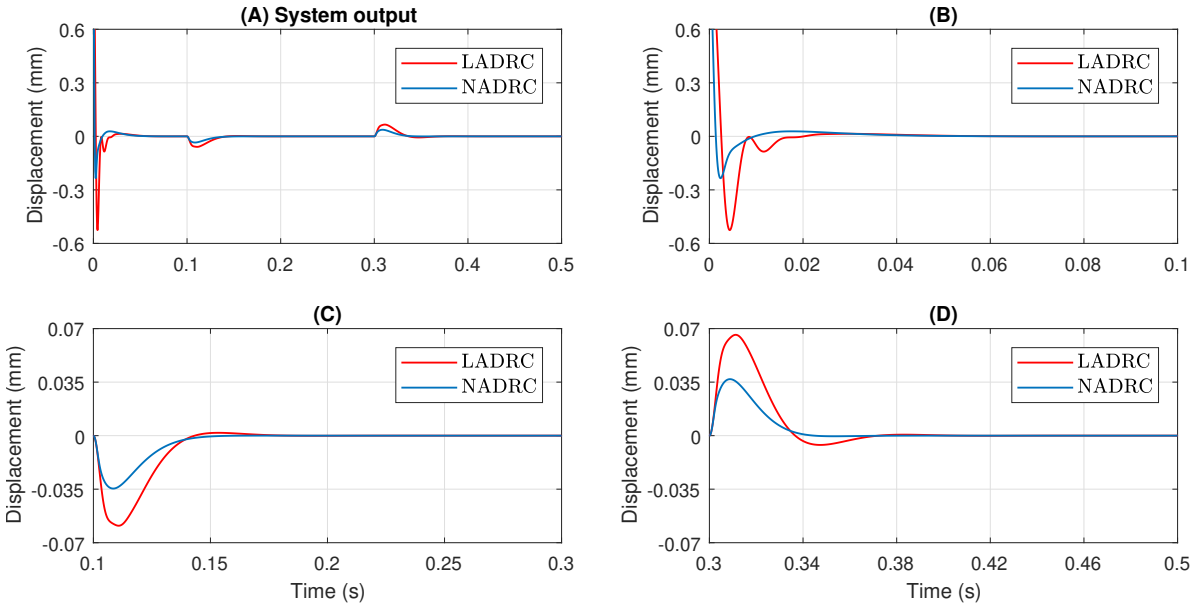

Figure 7: Plant response for LADRC and NADRC.

Figure 7(A) shows that both controllers corrected the plant output to the setpoint and were able to recover this condition even under a load change condition. Figures 7(B), 7(C) and 7(D) show a detailed view of the transitory regions. Figure 7 (B) indicates that the nonlinear model of ADRC can reach the reference faster and with less overshoot. Figures 7(C) and (D) are the response to the step external loads and indicates that the NADRC is more robust to disturbance.

The efficiency of the ADRC in controlling the output of the system depends directly on the ability of ESO to estimate the states of the plant, that is: $x_1 \rightarrow z_1$, $x_2 \rightarrow z_2$ e $F(t) \rightarrow z_3$. Figure 8 compares the dynamic response of the real states with their respective values estimated by the observer. It is clear the ability of the linear and nonlinear ESOs in providing proper estimations of the plant states.

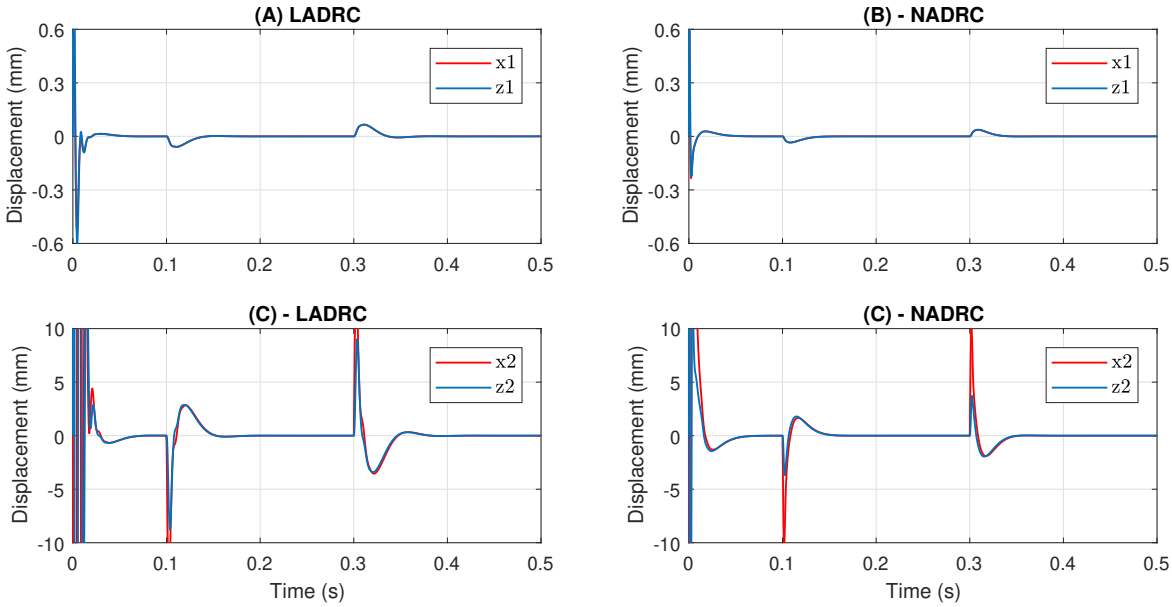

Figure 8: States estimation.

Figure 9 shows the generalized disturbance f and its estimation z_3. Despite some mismatch in the transitory period, the ESOs were successful in estimate the general behavior of the generalized disturbances.

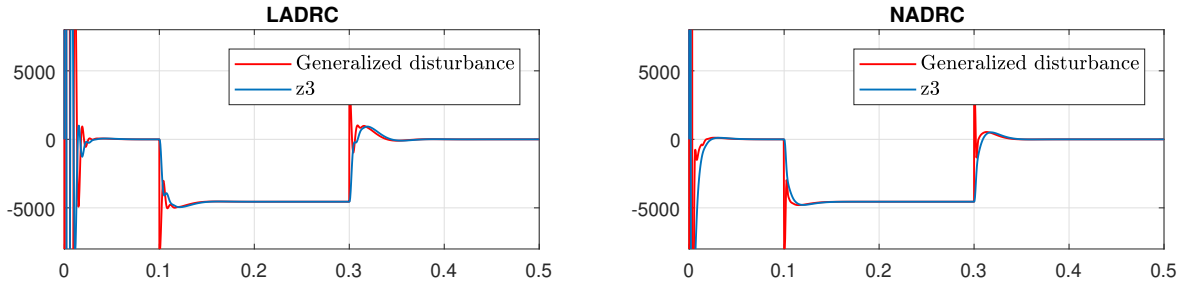

Figure 9: Generalized disturbance estimation.

5 Conclusions

This work studied the application of the ADRC technique to control a simulated plant that represent the rotor radial displacement of a bearingless machine with split winding.

From the simulated results, it was possible to notice that for both the linear and nonlinear controllers the ADRC was successful in providing a stable response to the system even in the presence of perturbations and parameters variations. Despite this, in a more precise point of view, the nonlinear ADRC structure presents a faster and more damped response when compared with the linear ADRC.

Since the performances for both controllers were similar, it is important to evaluate if it is necessary to use the NADRC, which is a more complex structure with more parameters to be tuned, instead of LADRC, which is easier to be built and tuned. Due the nonlinear nature of NADRC and the number of parameters of its implementation, in some cases researchers adopt optimization algorithms [14] instead of trial and error tuning. Again, it means an additional effort to use the NADRC technique that must be taken in account to make project decisions.

As the initial step of a project that aims to evaluate the ADRC to control a real prototype, this works provided the initial experience with this control paradigm and helped to test two different implementations of the ADRC. These results will be useful to future experimental implementations.

6 Acknowledgments

This work was supported by Comissão de Aperfeiçoamento de Pessoal do Nível Superior (CAPES), Programa de Pós-graduação em Engenharia Elétrica e de Computacão (PPgEEC/UFRN) and Conselho Nacional de Desenvolvimento Científico e Tecnológico (CNPq).

References

[1] Jiahao Chen and Eric L. Severson. Optimal design of the bearingless induction motor for industrial applications. In *2019 IEEE Energy Conversion Congress and Exposition (ECCE)*, pages 5265–5272, 2019.

[2] Jossana Maria de Souza Ferreira. Modelagem de máquina de indução trifásica sem mancais com bobinado dividido. 2006.

[3] Zhiqiang Gao. From linear to nonlinear control means: A practical progression. *ISA transactions*, 41(2):177–189, 2002.

[4] Zhiqiang Gao. Scaling and bandwidth-parameterization based controller tuning. In *Proceedings of the 2003 American Control Conference, 2003.*, volume 6, pages 4989–4996, 2003.

[5] Jingqing Han. From pid to active disturbance rejection control. *IEEE transactions on Industrial Electronics*, 56(3):900–906, 2009.

[6] Zhengjie Hao, Yang Yang, Yimin Gong, Zhengqiang Hao, Chenchen Zhang, Hongda Song, and Jiannan Zhang. Linear/nonlinear active disturbance rejection switching control for permanent magnet synchronous motors. *IEEE Transactions on Power Electronics*, 36(8):9334–9347, 2021.

[7] Deqing Huang, Da Min, Yupei Jian, and Yanan Li. Current-cycle iterative learning control for high-precision position tracking of piezoelectric actuator system via active disturbance rejection control for hysteresis compensation. *IEEE Transactions on Industrial Electronics*, 2019.

[8] Prashant Kumar, Abdul Rahiman Beig, Devara Vijaya Bhaskar, Khaled Ali Al Jaafari, Utkal Ranjan Muduli, and Ranjan kumar Behera. An enhanced linear active disturbance rejection controller for high performance pmbldcm drive considering iron loss. *IEEE Transactions on Power Electronics*, pages 1–1, 2021.

[9] Jie Li, Yuanqing Xia, Xiaohui Qi, and Zhiqiang Gao. On the necessity, scheme, and basis of the linear–nonlinear switching in active disturbance rejection control. *IEEE Transactions on Industrial Electronics*, 64(2):1425–1435, 2016.

[10] Ke Li, Guoyu Cheng, Xiaodong Sun, Dean Zhao, and Zebin Yang. Direct torque and suspension force control for bearingless induction motors based on active disturbance rejection control scheme. *IEEE Access*, 7:86989–87001, 2019.

[11] Yujun Liu, Hejin Xiong, and Heng Zhang. Research on active disturbance rejection control of active magnetic bearing-rotor system. In *2021 6th Asia Conference on Power and Electrical Engineering (ACPEE)*, pages 873–877, 2021.

[12] A.O. Salazar and R.M. Stephan. A bearingless method for induction machines. *IEEE Transactions on Magnetics*, 29(6):2965–2967, 1993.

[13] Eric Severson, Robert Nilssen, Tore Undeland, and Ned Mohan. Design of dual purpose no voltage combined windings for bearingless motors. In *2016 IEEE Energy Conversion Congress and Exposition (ECCE)*, pages 1–10, 2016.

[14] Suiyuan Shen and Jinfa Xu. Trajectory tracking active disturbance rejection control of the unmanned helicopter and its parameters tuning. *IEEE Access*, 9:56773–56785, 2021.

[15] Francisco Elvis Carvalho Souza. Otimização da estrutura de acionamento para o controle de posição radial de um motor de indução trifásico sem mancais com enrolamento dividido. 2018.

[16] Li Sun, Wenchao Xue, Donghai Li, Hongxia Zhu, and Zhi-gang Su. Quantitative tuning of active disturbance rejection controller for fopdt model with application to power plant control. *IEEE Transactions on Industrial Electronics*, pages 1–1, 2021.

[17] Xiaodong Sun, Long Chen, and Zebin Yang. Overview of bearingless induction motors. *Mathematical Problems in Engineering*, 2014, 2014.

[18] Thuy Vi Tran, Kyeong-Hwa Kim, and Jih-Sheng jason Lai. Optimized active disturbance rejection control with resonant extended state observer for grid voltage sensorless lcl-filtered inverter. *IEEE Transactions on Power Electronics*, pages 1–1, 2021.

[19] Zebin Yang, Jialei Ji, Xiaodong Sun, Huimin Zhu, and Qian Zhao. Active disturbance rejection control for bearingless induction motor based on hyperbolic tangent tracking differentiator. *IEEE Journal of Emerging and Selected Topics in Power Electronics*, 2019.

[20] Zebin Yang, Chengling Lu, Xiaodong Sun, Jialei Ji, and Qifeng Ding. Study on active disturbance rejection control of a bearingless induction motor based on an improved particle swarm optimization–genetic algorithm. *IEEE Transactions on Transportation Electrification*, 7(2):694–705, 2021.